ORIGINAL RESEARCH

Encapsulation of chloroquine and doxorubicin by MPEG-PLA to enhance anticancer effects by lysosomes inhibition in ovarian cancer

Ming Shao[1,*]
Weitao Zhu[2,*]
Xianping Lv[1]
Qiankun Yang[1]
Xin Liu[1]
Ying Xie[1]
Ping Tang[3]
Ling Sun[3]

[1]Department of Blood Transfusion, The First Affiliated Hospital of Zhengzhou University, Zhengzhou, Henan Province 450052, China; [2]Department of Clinical Laboratory, The First Affiliated Hospital of Zhengzhou University, Zhengzhou, Henan Province 450052, China; [3]Department of Hematology, The First Affiliated Hospital of Zhengzhou University, Zhengzhou, Henan Province 450052, China

*These authors contributed equally to this work

Correspondence: Ling Sun
Department of Hematology, The First Affiliated Hospital of Zhengzhou University, Jianshe Road, No 1, Erqi Square, Zhengzhou 450000, China
Tel +86 1 365 381 0185
Fax +86 1 365 381 0185
Email sunling6686@126.com

Purpose: As the deadliest gynecological malignancy, ovarian cancer ranks as a major cause of disease-related deaths to women worldwide and is treated with transurethral resection or systemic chemotherapy. However, traditional chemotherapeutic drug in antitumor therapy has shown unavoidable limitations, such as poor curative effects, systemic toxicity and development of drug resistance, leading to failure of tumor inhibition and recurrence. This study aims to explore an innovative method to enhance the clinical efficiency of ovarian cancer.

Materials and methods: Using MTT assay, the cell viability was detected under different culture systems. Western blot was used to examine the expression of P-gp in doxorubicin-resistant and wild-type A2780/SKOV3 cells. We used confocal to examine the drug concentration under different culture conditions. Also, flow cytometry was used to detect the drug absorption at the determined time points under different culture systems. Using nude mice model, we evaluated the killing efficacy of chemotherapeutic drugs with or without nanoparticle encapsulation. ELISA was used to examine the levels of creatinine, alanine aminotransferase and aspartate aminotransferase in plasma.

Results: We found that pretreatment of chloroquine (CQ) as chemosensitizer markedly enhanced the anticancer effects in ovarian cancer. We also provided evidence that CQ efficiently increase the pH value of lysosomes in tumor cells, leading to the reverse of drug sequestration induced by lysosomes. To further improve the pharmacokinetics profiles and avoid the systemic toxicity caused by chemotherapeutic agents, we encapsulated CQ and chemotherapeutic drugs by polymeric nanoparticles methoxy poly(ethylene glycol)-poly(L-lactic acid). Codelivery of CQ and chemotherapeutic agents by nanocarrier revealed enhanced anticancer effects compared with the free drug delivery by tail vein injection. More importantly, accumulated drugs, prolonged drug circulation and reduced organic damages were observed in nanoparticles delivery.

Conclusion: Codelivery of CQ and chemotherapeutic drugs by methoxy poly(ethylene glycol)-poly(L-lactic acid) could significantly improve the anticancer effects and might have important potency in clinical applications for ovarian cancer therapy.

Keywords: ovarian cancer, chloroquine, cisplatin, MPEG-PLA, nanoparticles

Introduction

With increasing incidence and mortality, ovarian cancer has been one of the most common malignancies with the leading cause of death in gynecological tumors.[1] Chemotherapy, one of the standard therapeutic regimens, has been proved to efficiently suppress the tumor growth and improve the outcome in ovarian cancer therapy. However, chemotherapeutic agents show poor responses to advanced metastatic carcinoma or recurrent tumors after chemotherapy, along with severe systemic toxicity and drug resistance development.[2,3] Hence, innovative approaches to enhance the anticancer

effects and reduce the potential systemic toxicity are the urgent needs in clinical ovarian cancer treatment.

Increasing evidence indicates that tumor cells could sequester chemotherapeutic drugs into lysosomes to prevent the interaction of agents and the targeted organelles, resulting in the reduced cytotoxicity and limited tumor suppression.[4] More importantly, the low pH value of lysosomes is capable of degrading the extraneous agents to avoid the cellular damages.[5] Chloroquine (CQ), a kind of 4-aminoquinoline drugs, has been reported to serve as the lysosomes inhibitors in tumor inhibition. Recent studies also indicated that CQ could increase the sensitivity of several tumor cells to chemotherapeutic agents, leading to the sensitization effects and enhanced anticancer effects. However, the potential systemic toxicity and low drug absorption in vivo limit the application of CQ in clinical tumor therapy.

Recently, the application of nanotechnology has efficiently improved the drug delivery system. Encapsulation of anticancer drugs by polymeric nanoparticles significantly facilitates the drug accumulation in tumor sites through an enhanced permeability and retention (EPR) and pH-dependent controlled release, resulting in better pharmacokinetics profiles and improved curative effects. Several micelles, such as methoxy poly(ethylene glycol)-poly(L-lactic acid) (MPEG-PLA) and methoxy polyglycol-polycaprolactone, has been attempted to deliver chemotherapeutic agents for enhanced anticancer effects and reduced toxicity caused by chemotherapy in vivo. Herein, we co-encapsulated CQ and doxorubicin (DOX) with MPEG-PLA polymer to form CQ/DOX co-encapsulated MPEG-PLA nanoparticles (CQ-DOX/MPEG-PLA). Codelivery of CQ and DOX by MPEG-PLA nanoparticles revealed dramatic tumor suppression while significantly reducing the toxicity induced by CQ and DOX. Our results suggest that the codelivery of CQ and DOX by MPEG-PLA nanoparticles has a potential application in ovarian cancer therapy.

Materials and methods
Cell lines and regents
MPEG-PLA (MPEG:PLA molar ratio =50:50, molecular weight =4,000 g/mol) was purchased from Daigang (Jinan, China). DOX, cis-platinum (DDP), paclitaxel (PTX), verapamil and CQ were purchased from Sigma (San Francisco, CA, USA). Human ovarian cancer cells A2780 and SKOV3 were purchased from American Type Culture Collection (Rockville, MD, USA) and supplemented with RPMI-1640 complete culture medium (Gibco, Carlsbad, CA, USA) containing 10% fetal calf serum (Gibco), at 37°C in a 5% CO_2 atmosphere. The DOX-resistant ovarian cancer cell

lines A2780/DOX[R] were established by culturing cells with DOX in a dose-escalation manner using long-term exposure intervals. Initial cultures of A2780 were supplemented with 10 nM DOX. After sensitive clones were no longer present and surviving A2780 cells repopulated the flask, the concentration of DOX was increased to 25, 50, 100, 200 and 500 nM. The process of acquired drug resistance took 4 months for A2780/DOX[R] cells.

Cell viability detection
Cell viability was determined by MTT assay kit (Solarbio, Beijing, China). Briefly, 3,000 cells were seeded into 96-well culture plates for 12 hours to adhere. Cells were treated with or without 10 µM CQ for 2 hours. Next, the cells were treated with different concentration of chemotherapeutic agents for 48 hours. Finally, cell growth was measured after addition of 10 µL 0.5 mg/mL MTT solution. After 4 hours of incubation at 37°C, the medium was replaced with 100 µL dimethylsulfoxide and vortexed for 10 minutes. Absorbance (A) was measured at 570 nm by a microplate reader (Bio-Rad, Irvine, CA, USA).

Western blot
Whole cell lysates were prepared from A2780 and A2780/DOX[R] cells and separated by SDS-PAGE at 100 V for 2 hours. Separated proteins were then transferred to nitrocellulose membranes (EMD Millipore, Billerica, MA, USA). The membranes were blocked in 5% BSA in TBST for 1 hour at room temperature. Then, the membranes were incubated with anti-P-gp antibody (Abcam, 1:500, Cambridge, UK) or anti-β-actin antibody (Abcam, 1:1,000) overnight at 4°C. The membranes were washed three times and incubated with horseradish peroxidase-conjugated secondary antibodies (Abcam, 1:1,000). Proteins were visualized by ECL Western blotting substrate (Thermo Fisher Scientific, Waltham, MA, USA).

Lysosome pH detection
The lysosome pH of A2780 cells (pretreated with 10 µM CQ for 2 hours or not) were detected by Intracellular pH Calibration Buffer Kit (Thermo Fisher Scientific) as previous. Briefly, after washing A2780 cells with Live Cell Imaging Solution, one-fourth Live Cell Imaging Solution was replaced with the 1 mM Cell Loading Solution with Valinomycin/Nigericin and was incubated at 37°C for 5 minutes. Then, the samples were analyzed using appropriate Ex/Em maxima. We also used lysosome sensor to analyze the lysosome pH influence by Confocal (Olympus Corporation, Tokyo, Japan). Briefly, A2780 cells were pretreated with CQ (10 µM,

2 hours), then 1 mM Lyso-Sensor was added into the culture system. After 30 minutes, the cells were analyzed with a confocal microscope (Olympus Corporation).

Confocal microscopy analysis

To illustrate the mechanism of CQ sensitizing the tumor cells, tumor cells were incubated with DOX at 37°C for different periods of time after pretreated with/without 10 µM CQ for 2 hours. After fixed and permeabilized, the cells were blocked with 5% BSA in PBS and incubated with primary antibody against LAMP2 (Abcam, 1:100) or P-gp (Abcam, 1:200) overnight at 4°C. Sections were then incubated with fluorescence-labeled secondary antibody (1:1,000, Life Technologies, Camarillo, CA, USA), followed by counterstaining with DAPI (Solarbio, Beijing, China). Images were captured with a confocal microscope (Olympus Corporation).

siRNA interference

A2780 cells ($3×10^5$) were seeded in six-well plates and cultured in 37°C. After 24 hours, the transfection reagent and siRNA complex or control vector were added to the culture system, followed by designed treatment. Human siRNAs against transcription factor EB (TFEB) was used 5′-GACG AAGGUUCAACAUCAA-3′.

Preparation of DOX/PTX/DDP and CQ-loaded nanoparticles

DOX- and CQ-loaded MPEG-PLA nanoparticles preparation: 95 mg MPEG-PLA, 1.5 mg DOX (or 4.2 mg PTX or 1.8 mg DDP) and 1.5 mg CQ were co-dissolved in 2 mL dichloromethane, followed by evaporation under reduced pressure in a rotary evaporator at 60°C. Next, the film was rehydrated in 500 mL PBS (pH =7.4), allowing the self-assembly of nanoparticles.

Drug loading (DL) and encapsulation efficiency (EE) of codelivery nanoparticles were calculated from the following formulas:

$$DL = \frac{\text{Weight of drug in nanoparticles}}{\text{Weight of nanoparticles}}.$$

$$EE = \frac{\text{Weight of drug in nanoparticles}}{\text{Weight of drug total used}}.$$

Particle size analysis and morphology study

The particle size, polydispersity index and zeta potential of nanoparticles were detected by Malvern Nano ZS90 (Malvern

Instruments, Malvern, UK). The measuring progress was carried out under the temperature of 25°C. The morphology of the prepared nanoparticles was studied with transmission electron microscope (Hitachi Ltd., Tokyo, Japan). Briefly, distilled water was used to dilute the nanoparticles, and the samples were placed on a copper grid covered with nitrocellulose. Samples were negatively stained with phosphotungstic acid and dried at room temperature.

Drug release study

In vitro drug release behaviors of DOX and CQ in nanoparticles were determined by a dialysis method. Briefly, 2 mL DOX or CQ in PBS, and DOX- and CQ-loaded MPEG-PLA nanoparticles were placed in dialysis bags (molecular weight cutoff, 3.5 kDa). The dialysis bags were incubated in 20 mL PBS containing 2 mL FBS (37°C and pH =5.0 or 7.4) in a 50 mL tube with shaking at 100 rpm. At predetermined time points, 2 mL of release media was collected for further analysis, and the incubation medium needs to be replaced with fresh incubation medium. The amount of released drugs was quantified by HPLC (Waters 2695; Waters Corporation, Milford, MA, USA). Analysis of CQ was carried out using a Varian HPLC system equipped with a ternary pump Model 9012 and UV Diode Array Detector Model 9065. A Lichrospher 60 RP-select B column (250×4 mm I.D., 5 µm particle size) with the analogous guard column (4×4 mm, 5 µm particle size) was used in our experiment. Isocratic elution was performed with a flow rate of 1 mL/min at ambient temperature. For DOX, the HPLC system consisted of a 1525 Binary HPLC Pump, a 717 Plus Autosampler and a 2475 Multi-Wavelength Fluorescence Detector (Waters Corporation). Chromatography was performed on a column (4.6250 mm, particle size 5 mm). The effluents were monitored at an excitation wavelength of 480 nm and an emission wavelength of 560 nm at 35°C. Detection and integration of chromatographic peaks were performed using Empower 2 software (Waters Corporation).

Animal protocol

For mouse model, nude mice were subcutaneously transplanted $2×10^6$ A2780 (or SKOV3, or A2780/DOX^R) cells. When the tumor volume reaching 70 mm³, PBS, CQ (5 mg/kg), DDP (6 mg/kg) or DDP (6 mg/kg) combining with CQ (5 mg/kg), PP (MPEG-PLA) and DOX/PP (DOX 5 mg/kg) were injected by cauda vein every 3 days for 4 weeks. Tumor growth was recorded with the length (L) and width (W) of tumors by vernier calipers, and the tumor volume (V) was calculated by the formula $V = (L×W^2/2)$.

For the systemic toxicity analysis, normal C57 mice or tumor-bearing mice (mice were treated when the tumor volume reaching 70 mm^3) were treated with PBS, DOX (5 mg/kg) combined with CQ (5 mg/kg) and DOX-CQ/PP (DOX 5 mg/kg and CQ 5 mg/kg) every 2 days for 24 days. The weight of mice was recorded every day. After 24 days, the mice were sacrificed for the aspartate aminotransferase/ glutamic oxalacetic transaminase (AST/GOT), alanine aminotransferase/glutamic-pyruvic transaminase (ALT/GPT) and creatinine (CRE) analysis as guided.

For drug distribution detection, nude mice were subcutaneously transplanted 2×10^6 A2780 cells. When the tumor volume reaching 3×3 mm, mice were grouped and received PBS, DOX (5 mg/kg) combined with CQ (5 mg/kg) and DOX-CQ/PP (DOX 5 mg/kg and CQ 5 mg/kg) every 2 days for 10 days. Then, the mice were sacrificed, and the tumor, urine, serum and the organs were obtained. HPLC was used to examine the DOX concentration in samples.

Statistical analysis

Results were presented as mean ± SEM, and statistical significance was examined by an unpaired Student's *t*-test (for animal survival analysis) and one-way ANOVA by the GraphPad 6.0 software. *P*-value <0.05 was considered as statistically significant.

Results
CQ sensitized the ovarian cancer cells to chemotherapeutic drugs in vitro

Currently, increasing evidence has shown that CQ could enhance the killing efficacy of chemotherapeutic drugs to multiple tumor cells.[6,7] However, the underlying mechanism of the sensitization effect remains unclear. To further investigate the potential curative effects of CQ in ovarian cancer treatment and the specific mechanism, we treated ovarian cancer cell lines A2780 and SKOV3 with different doses of CQ (5/10/20/50/100/200 μM) and then detected the cell viability. However, we observed that CQ had limited inhibition of cell growth in both A2780 (Figure 1A) and SKOV3 (Figure 1B) cells under lower concentrations (<20 μM) (Figure 1A and B). Recent studies revealed that CQ could serve as an effective sensitizer to enhance the curative effects of chemotherapy instead of killing the tumor cells directly.[7] Herein, we used DOX, PTX and DDP, three chemotherapeutic drugs for ovarian cancer treatment in clinic, to investigate the potential role of CQ to sensitize ovarian cancer cells to chemotherapy. We pretreated A2780 and SKOV3 cells with low dose CQ (10 μM), followed by

gradient doses of DOX. We found that CQ pretreatment could significantly enhance the killing efficacy of DOX in both A2780 (Figure 1C) and SKOV3 cells (Figure 1D) compared with DOX alone treatment. Besides, enhanced killing ability of PTX (4 μM for A2780 and 40 nM for SKOV3 cells) (Figure 1E) and DDP (20 μM for both A2780 and SKOV3 cells) (Figure 1F) combining with CQ (10 μM) were observed compared with drug treatment alone, demonstrating that CQ could significantly elevate the sensitivity of ovarian cancer cells to chemotherapy.

Recently, the development of multidrug resistance remains to be a hurdle in clinical ovarian cancer therapy.[8] To further investigate whether CQ could sensitize the drug-resistant ovarian cancer cells to chemotherapeutic agents, we established DOX-resistant A2780 cells (Figure 1G). Increasing evidence has shown that P-gp works as an important player to develop drug resistance in a variety of cancers.[9] Here, we observed enhanced P-gp expression in A2780/DOX^R cells compared with that in wild-type A2780 cells (Figure 1H). Intriguingly, pretreatment of CQ (10 μM) could significantly enhance A2780/DOX^R cell apoptosis induced by DOX (Figure 1I), indicating the sensitization effect of CQ could also be observed in drug-resistant ovarian cancer cells. Together, these data suggested that CQ could efficiently facilitate the killing ability of chemotherapeutic drugs to ovarian cancer cells by a sensitization effect.

CQ sensitized the ovarian cancer cells to chemotherapy through reversing the drug sequestration of lysosomes

Next, we explored the potential mechanism of CQ to sensitize ovarian cancer cells. In fact, increasing evidence revealed that lysosomes in tumors could efficiently segregate extraneous agents and degrade various compounds via its lower pH value.[10] CQ, a 4-aminoquinoline drug, has been reported to be capable of suppressing the lysosomes functions.[11] To investigate whether CQ sensitizes ovarian cancer cells in a lysosome-dependent way, we treated A2780 cells with DOX (4 μM) pretreated with or without CQ (10 μM) and then detected the drug distribution and lysosomes in cancer cells by confocal. Intriguingly, we observed higher concentration of DOX in the nuclear of CQ pretreated A2780 cells, while accumulated DOX in lysosomes was found in PBS group (Figure 2A). Considering the inhibition function of CQ to lysosome, we supposed that the lysosomes in tumor cells might be capable of segregating the extraneous agents and the treatment of CQ release the isolated drugs from lysosomes, resulting in the chemotherapy sensitization. To further
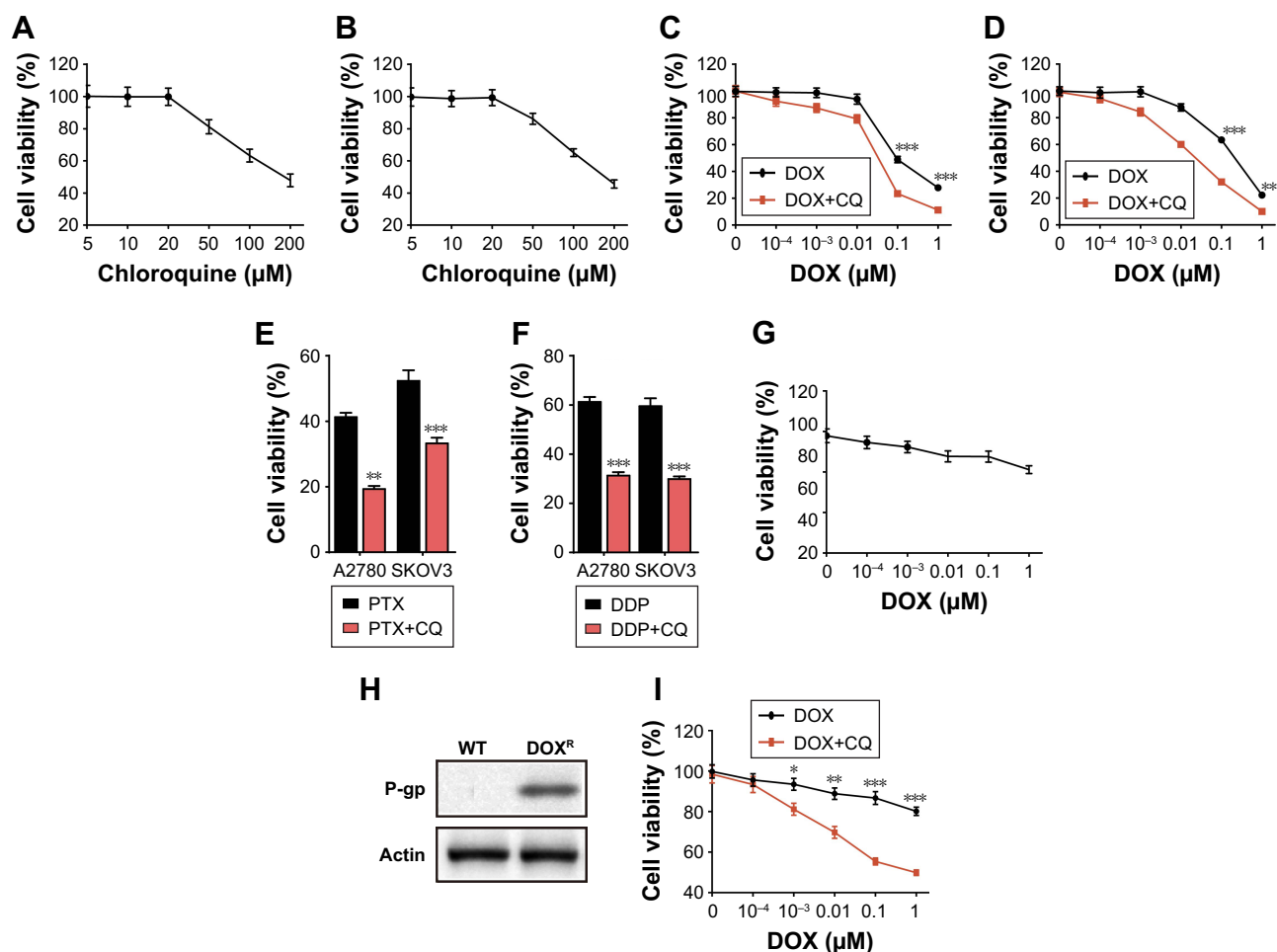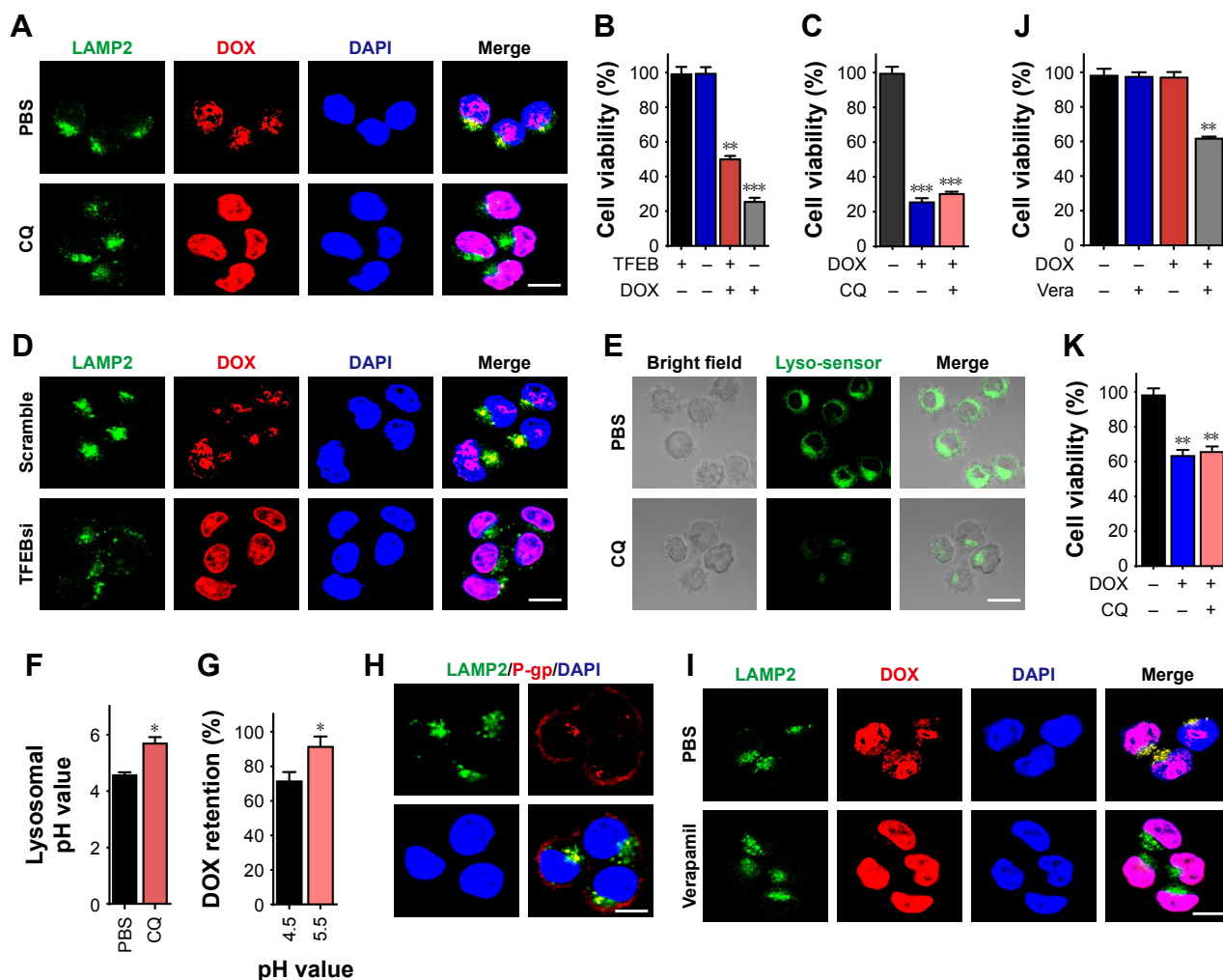
Figure 1 CQ sensitized the ovarian cancer cells to chemotherapeutic drugs in vitro.

Notes: (**A**) Cell viability of A2780 cells was analyzed by MTT methods after treatment with gradient doses of CQ (5/10/20/50/100/200 μM) for 48 hours. (**B**) Cell viability of SKOV3 cells was analyzed by MTT methods after treatment with gradient doses of CQ (5/10/20/50/100/200 μM) for 48 hours. (**C**) Cell viability of A2780 cells was analyzed by MTT methods after treatment with gradient doses of DOX (0.0001/0.001/0.01/0.1/1 μM) pretreated with or without CQ (10 μM, 2 hours) for 48 hours. (**D**) Cell viability of SKOV3 cells was analyzed by MTT methods after treatment with gradient doses of DOX (0.0001/0.001/0.01/0.1/1 μM) pretreated with or without CQ (10 μM, 2 hours) for 48 hours. (**E**) Cell viability of A2780 and SKOV3 cells was analyzed by MTT methods after treatment with PTX (4 μM for A2780 and 40 nM for SKOV3 cells) pretreated with or without CQ (10 μM, 2 hours) for 48 hours. (**F**) Cell viability of A2780 and SKOV3 cells was analyzed by MTT methods after treatment with DDP (20 μM for both A2780 and SKOV3 cells) pretreated with or without CQ (10 μM, 2 hours) for 48 hours. (**G**) Cell viability of A2780/DOX^R cells was analyzed by MTT methods after treatment with gradient doses of DOX (0.0001/0.001/0.01/0.1/1 μM) for 48 hours. (**H**) Using Western blot, we examined the expression of P-gp in wild-type and DOX-resistant A2780 cells. (**I**) Cell viability of A2780/DOX^R cells was analyzed by MTT methods after treatment with gradient doses of DOX (0.0001/0.001/0.01/0.1/1 μM) pretreated with or without CQ (10 μM) for 48 hours. *$P < 0.05$; **$P < 0.01$; ***$P < 0.001$.

Abbreviations: CQ, chloroquine; DOX, doxorubicin; ns, no significant difference; PTX, paclitaxel; ET, wild type.

demonstrate the relationship between the lysosomes and the sensitization effects induced by CQ, we silenced the TFEB, the master regulator for lysosomal biogenesis, and examined the TFEB silenced A2780 cell viability with or without DOX treatment. We found that DOX (0.1 μM) induced stronger killing efficiency to TFEB silenced A2780 cells compared with the mock group (Figure 2B). Furthermore, pretreatment of CQ (10 μM) showed no sensitizing effect on TFEB silenced A2780 cells to DOX (0.1 μM) (Figure 2C), indicating that CQ sensitizes the ovarian cancer cells to chemotherapeutic agents in a lysosome-associated pathway. In addition, silence of TFEB in A2780 released the DOX from lysosomes, leading to elevated concentration of

DOX in nucleus, which was consistent with our hypothesis (Figure 2D). Next, we wondered how CQ sensitized the cancer cells through the lysosomes. The acidic environment of lysosomes is the basis for the cellular lysosomes to resolve the cellular debris or extraneous materials via hydrolase enzymes.[12] Intriguingly, we observed that CQ (10 μM) treatment increased the lysosomal pH value from 4.5 to 5.5 in A2780 cells (Figure 2E and F). Various studies have revealed that the metabolism of chemotherapeutic agents was intimately correlated with the pH value.[13] Thus, we examined the degradation of DOX under different pH conditions. Normalized to the pH 4.5 environment, DOX degradation was reduced as the pH value raised (Figure 2G), indicating that CQ could increase

Figure 2 CQ sensitized the ovarian cancer cells to chemotherapy through reversing the drug sequestration of lysosomes.
Notes: (**A**) A2780 cells were treated with DOX (4 μM, 4 hours) pretreated with or without CQ (10 μM, 2 hours), followed by LAMP2 staining. The result was analyzed under two-photon confocal microscope. Scale bar, 10 μm. (**B**) The cell viability of A2780 cells knocking down TFEB after treated with 0.1 μM DOX for 48 hours. (**C**) The cell viability of SKOV3 cells knocking down TFEB after treated with 0.1 μM DOX for 48 hours pretreated with or without CQ (10 μM, 2 hours). (**D**) Silencing TFEB or mock A2780 cells were treated with DOX (4 μM) for 4 hours, followed by LAMP2 staining. The result was analyzed under two-photon confocal microscope. Scale bar, 10 μm. (**E**) A2780 cells were treated with or without CQ (10 μM, 2 hours), followed by stained with lysosome sensor (1 μM) for 30 minutes. The result was analyzed under two-photon confocal microscope. Scale bar, 10 μm. (**F**) The lysosomal pH values of A2780 cells treated with or without CQ (10 μM) for 2 hours. (**G**) The metabolisms of DOX under different pH conditions were examined by HPLC. (**H**) The co-locations of LAMP2 and P-gp in A2780/DOX^R cells were analyzed by using two-photon confocal microscope. Scale bar, 10 μm. (**I**) A2780/DOX^R cells were pretreated with or without verapamil (5 μM, 2 hours), followed by DOX treatment (4 μM, 4 hours). The cells were stained with LAMP2 and analyzed under two-photon confocal microscope. Scale bar, 10 μm. (**J**) The cell viability of A2780/DOX^R cells was detected after DOX (0.1 μM) treatment with or without verapamil (5 μM, 2 hours). (**K**) The cell viability of A2780/DOX^R cells was measured after DOX treatment with or without CQ (10 μM, 2 hours). *$P < 0.05$; **$P < 0.01$; ***$P < 0.001$.
Abbreviations: CQ, chloroquine; DOX, doxorubicin; ns, no significant difference; TFEB, transcription factor EB.

the lysosome pH value to reverse the acidic environment, resulting in the reduced degradation of chemotherapeutic agents in tumor cells. However, it still remained unclear that the accumulation of agents in lysosomes in tumor cells and the release of drugs from lysosomes induced by CQ in our previous result (Figure 2A). It has been reported that P-gp, a member of ABC transporter expressed in the cell membranes and lysosomal membranes, is capable of pumping extraneous drugs from cytoplasm into lysosomes, leading to the drug sequestration in lysosomes.[14] Previously, we have observed that the pretreatment of CQ increased the lysosomal pH value.

It has been well illustrated that the pH increase could induce inactivation of P-gp in lysosomal membrane and finally result in the drug efflux from lysosomes. Here, we employed A2780/DOX^R cells as model for further investigation. We detected the expression of P-gp and LAMP2 (the protein marker of lysosomes) in A2780/DOX^R cells and observed co-location of P-gp and lysosomes (Figure 2H), indicating that the expression of P-gp in A2780 cells lysosomes. To testify the role of P-gp in reversing drug sequestration induced by CQ, we used verapamil, a P-gp inhibitor, to pretreat the A2780/DOX^R cells. Next, we treated A2780/DOX^R with DOX (4 μM).

Pleasantly, release of DOX from lysosomes was observed after verapamil (5 µM) treatment (Figure 2I). Moreover, pretreatment of verapamil (5 µM) also facilitated the cytotoxicity of DOX (0.1 µM) to A2780/DOX^R cells (Figure 2J) and reverse the sensitization effect induced by CQ (10 µM) (Figure 2K), indicating that the CQ increase the lysosome pH values, leading to the inactivation of P-gp and reverse of drug sequestration in lysosomes. Together, these results suggested that CQ could efficiently reduce the drug degradation and reverse the drug sequestration induced by P-gp in lysosomes through increasing lysosomal pH, resulting in the chemotherapy sensitization.

Combination of CQ and chemotherapeutic drugs inhibited the tumor growth in ovarian cancer mice model along with organ damage

To assess the killing efficiency of CQ in combination with chemotherapeutic agents, nude mice models bearing A2780 and SKOV3 cells were constructed. Upon tumor volume reaching 70 mm³, the mice were randomly divided into four groups. The treatments were applied as following: control groups (PBS), drugs alone (DDP 6 mg/kg, PTX 15 mg/kg and DOX 5 mg/kg), CQ alone (5 mg/kg) and CQ combined with drugs (DDP 6 mg/kg, PTX 15 mg/kg and DOX 5 mg/kg). The tumor volume was measured every day, and the death time was recorded in all groups. According to the data, we observed that the tumor volume in CQ alone treatment group showed

similar growth rate compared with control group. DDP treatment showed limited tumor growth inhibition compared with the control group, and combination of CQ and DDP exhibited significant tumor remission in mice models bearing A2780 cells (Figure 3A, left). Correspondingly, we found that the survival time of mice in CQ alone treatment showed no difference with those in the control group. DDP alone exhibited limited efficacy on survival time of mice, while combination of DDP and CQ treatment significantly prolonged the survival time in A2780 mice models (Figure 3A, right), reminding that CQ combining with DDP could significantly remiss tumor growth and prolong the survival time. Apart from DDP, we also evaluated the efficacy of CQ combined with PTX and DOX to treat A2780 mice models. And we found that PTX (Figure 3B, left) or DOX (Figure 3C, left) alone exhibited limited inhibition of tumor volume in mice bearing A2780 cells, and combination of PTX (or DOX) and CQ significantly prolonged the survival time (Figure 3B and C, right). Besides, we also used DDP, PTX and DOX with or without CQ to treat mice bearing SKOV3 cells obtained similar results in tumor volume inhibition and survival time (Figure 3D–F). These data suggested that CQ could significantly enhance the killing ability of chemotherapy and prolong survival time in ovarian cancer mice models. Our previous data showed that CQ could significantly reverse the drug resistance in vitro. To further investigate the potential role of CQ in mice models bearing drug-resistant ovarian cancer cells, we established A2780/DOX^R mice models. We found that DOX exhibited no
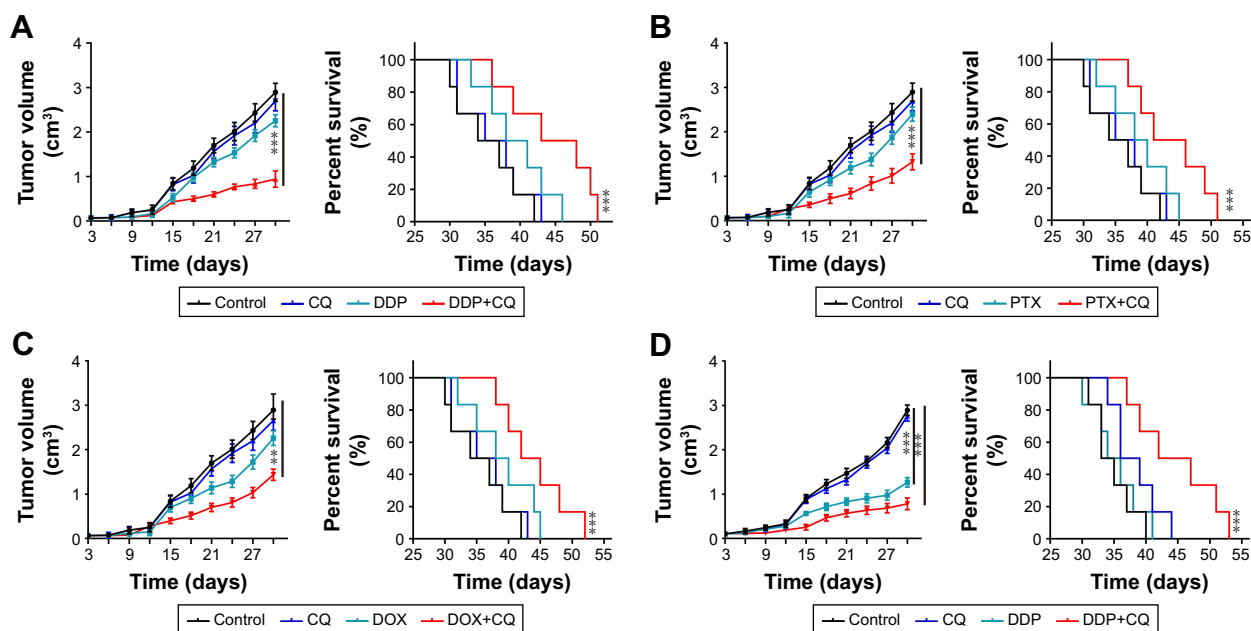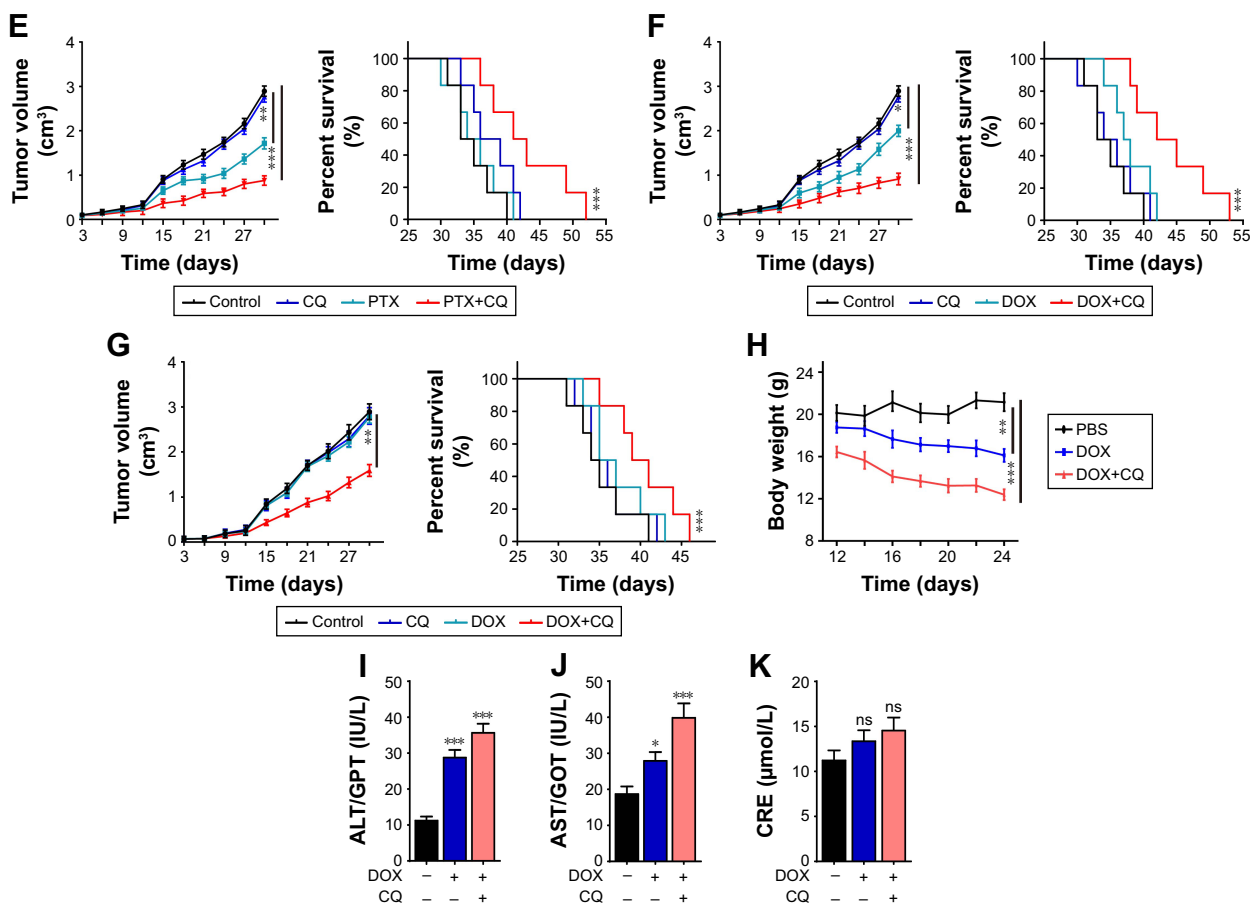

Figure 3 (*Continued*)

Figure 3 CQ combined with chemotherapeutic drugs inhibited the tumor growth in ovarian cancer mice model along with organ damage.
Notes: (**A**) Tumor volume of nude mice model bearing A2780 cells treated with PBS, CQ (5 mg/kg), DDP (6 mg/kg) or DDP (6 mg/kg) combining with CQ (5 mg/kg) were measured (n=6) (left). Survival time of nude mice model bearing A2780 cells treated with PBS, CQ (5 mg/kg), DDP (6 mg/kg) or DDP (6 mg/kg) combining with CQ (5 mg/kg) in each group (n=6) (right). (**B**) Tumor volume of nude mice model bearing A2780 cells treated with PBS, CQ (5 mg/kg), PTX (15 mg/kg) or PTX (15 mg/kg) combining with CQ (5 mg/kg) were measured (n=6) (left). Survival time of nude mice model bearing A2780 cells treated with PBS, CQ (5 mg/kg), PTX (15 mg/kg) or PTX/PP (15 mg/kg) combining with CQ (5 mg/kg) in each group (n=6) (right). (**C**) Tumor volume of nude mice model bearing A2780 cells treated with PBS, CQ (5 mg/kg), DOX (5 mg/kg) or DOX (DOX 5 mg/kg) combining with CQ (5 mg/kg) were measured (n=6) (left). Survival time of nude mice model bearing A2780 cells treated with PBS, CQ (5 mg/kg), DOX (5 mg/kg) or DOX (5 mg/kg) combining with CQ (5 mg/kg) in each group (n=6) (right). (**D**) Tumor volume of mice model bearing SKOV3 cells treated with PBS, CQ (5 mg/kg), DDP (6 mg/kg) or DDP (6 mg/kg) combining with CQ (5 mg/kg) were measured (n=6) (left). Survival time of mice model bearing A2780 cells treated with PBS, CQ (5 mg/kg), DDP (6 mg/kg) or DDP (5 mg/kg) combining with CQ (5 mg/kg) in each group (n=6) (right). (**E**) Tumor volume of nude mice model bearing SKOV3 cells treated with PBS, CQ (5 mg/kg), PTX (15 mg/kg) or PTX (15 mg/kg) combining with CQ (5 mg/kg) were measured (n=6) (left). Survival time of nude mice model bearing A2780 cells treated with PBS, CQ (5 mg/kg), PTX (15 mg/kg) or PTX (15 mg/kg) combining with CQ (5 mg/kg) in each group (n=6) (right). (**F**) Tumor volume of nude mice model bearing SKOV3 cells treated with PBS, CQ (5 mg/kg), DOX (5 mg/kg) or DOX (5 mg/kg) combining with CQ (5 mg/kg) were measured (n=6) (left). Survival time of nude mice model bearing A2780 cells treated with PBS, CQ (5 mg/kg), DOX (5 mg/kg) or DOX (5 mg/kg) combining with CQ (5 mg/kg) in each group (n=6) (right). (**G**) Tumor volume of nude mice model bearing A2780/DOX^R cells treated with PBS, CQ (5 mg/kg), DOX (5 mg/kg) or DOX (5 mg/kg) combining with CQ (5 mg/kg) were measured (n=6) (left). Survival time of nude mice model bearing A2780 cells treated with PBS, CQ (5 mg/kg), DOX (5 mg/kg) or DOX (5 mg/kg) combining with CQ (5 mg/kg) in each group (n=6) (right). (**H**) The body weight of C57 mice was measured in control, DOX and DOX-CQ groups (n=6). (**I**) The levels of alanine aminotransferase/glutamic-pyruvic transaminase (ALT/GPT) were detected in C57 mice received DOX (5 mg/kg) with or without CQ (5 mg/kg) (n=6). (**J**) The levels of aspartate aminotransferase/glutamic oxalacetic transaminase (AST/GOT) were detected in C57 mice received DOX (5 mg/kg) with or without CQ (5 mg/kg). (**K**) The concentrations of CRE were detected in C57 mice received DOX (5 mg/kg) with or without CQ (5 mg/kg). PP was short for MPEG-PLA. *$P<0.05$; **$P<0.01$; ***$P<0.001$.
Abbreviations: CRE, creatinine; CQ, chloroquine; DOX, doxorubicin; ns, no significant difference; PTX, paclitaxel.

significant tumor remission or obviously prolonged survival time, while combination of DOX and CQ could significantly inhibit tumor growth and prolong survival time of mice bearing A2780/DOX^R cells (Figure 3G). Together, these results reminded that CQ could enhance the efficacy of chemotherapy.

Although chemotherapy could inhibit the tumor growth and prolong survival time to some extent, it is always

accompanied with severe organ damage. In fact, the side effects induced by chemotherapy has become an obstacle for chemotherapy, including hypersensitivity reactions, and myelosuppression.[15] In this study, we assessed the systemic toxicity of DOX combined with CQ in healthy C57 and tumor-bearing nude mice. The DOX was applied to mice every 2 days and then we collected blood after last treatment. We observed obvious weight loss in DOX

(5 mg/kg) and DOX combined with CQ (5 mg/kg) groups (Figure 3H). We also detected the chemical reactions in the serum and observed that single DOX induced clear damage on the liver (Figure 3I and J), while had limited damage on kidney (Figure 3K) functions. Also, we constructed nude mice models bearing A2780 cells and assessed the systemic toxicity of DOX combined with CQ. According to the data, the weight loss was observed in DOX (5 mg/kg) and DOX combined with CQ (5 mg/kg) groups as well as in control group (Figure S1A). We also detected the chemical reactions in the serum and observed that single DOX or combing with CQ induced clear damage on the liver (Figure S1B and C), while had limited damage on kidney (Figure S1D) functions. Above, these results suggested that CQ could significantly enhance the killing ability of chemotherapeutic drugs in vivo, while induced with unavoidable systemic toxicity.

MPEG-PLA nanoparticles encapsulated CQ- and DOX-induced enhanced cell apoptosis in vitro and reduced drug accumulation in organs in vivo

Recently, nanoparticles have attracted increasing attention for the dramatic enhanced anticancer effects and reduced systemic toxicity in chemotherapy.[16] It has been reported that encapsulation of anticancer drugs by nanoparticles could efficiently deliver drugs to tumor sites through an EPR effect and superior pharmacokinetics profiles in vivo, resulting in prolonged drug circulation and reduced systemic toxicity in vivo.[17] MPEG-PLA nanoparticles show high EE, stability and low clearance, which make it as a promising delivery tool for chemotherapeutic drugs. The amphiphilic property of MPEG-PLA enables the nanoparticles to self-assemble to be micelles and form a core–shell structure during the process of rehydration.[18] In our studies, evaporation of the DOX, CQ and MPEG-PLA co-dissolved solution allowed the several components adequately mixed to form DOX-CQ/PP nanoparticles. The size of the DOX-CQ/PP nanoparticles used in this study was −25 nm (Figure 4A). Furthermore, nanoparticles with a size below 100 nm are easy for mammalian cells to uptake, which makes the MPEG-PLA nanoparticles appropriate for drug delivery. The transmission electron microscopic image of DOX-CQ/PP nanoparticles was shown in Figure 4B. Our nanoparticles revealed a polydispersity index of 0.163 with a zeta potential of −23.4 mV (Figure 4C), indicating a high uniformity and stability. The release of drugs encapsulated by nanoparticles is an important factor to evaluate and is affected by pH value. So, we examined the release of DOX and CQ encapsulated

in nanoparticles under different pH conditions via dialysis method. And we observed that both DOX (Figure 4D) and CQ (Figure 4E) released slower from nanoparticles compared with free drugs. To note, MPEG-PLA nanoparticles released the loaded drugs more effectively in the acidic condition (pH −5.5) compared with physiological conditions (pH −7.4) (Figure 4D and E). These data suggested that MPEG-PLA nanoparticle can preserve chemotherapeutic agents in physiological condition (pH −7.4), while selectively releasing them in tumor tissue (pH −5.5) by sensing the pH environment. Apart from DOX, we also encapsulated PTX and DDP and examined the EE and DL. As shown in Figure 4F, the nanoparticles have an EE of 95.36% (DOX), 93.73% (PTX) and 92.14% (DDP), and DL of 3.32% (DOX), 4.01% (PTX) and 2.34% (DDP), respectively. Furthermore, we evaluated the drug delivery efficiency of MPEG-PLA nanoparticles. We found that MPEG-PLA encapsulated DOX could significantly elevate the drug concentration in A2780 cells compared with DOX treatment, while MPEG-PLA co-encapsulating DOX and CQ resulted in the most accumulation of DOX in A2780 cells (Figure 4G). Correspondingly, the same result was observed in A2780 cells (Figure 4H). These data suggested that MPEG-PLA encapsulation could elevate DOX accumulation, and co-encapsulation of DOX and CQ by MPEG-PLA could significantly enhance drug absorption by ovarian cancer cells. The cytotoxicity of chemotherapy is positively correlated with the accumulation in cancer cells. Thus, we examined the cell viability of MPEG-PLA encapsulating DOX and CQ. We observed that DOX-CQ/PP treatment induced serve cells apoptosis compared with DOX/PP treatment or DOX treatment in A2780 cells (Figure 4I). Similar results were obtained when tested with DDP (Figure 4J) and PTX (Figure 4K), indicating that MPEG-PLA encapsulation could induce higher toxicity of chemotherapeutic agents to ovarian cancer cells. Furthermore, we observed that DOX-CQ/PP could also significantly sensitize A2780/DOX[R] cells (Figure 4L), indicating that MPEG-PLA encapsulating DOX and CQ could also reverse drug resistance in drug-resistant cancer cells, which is in line with our previous result. To further investigate the drug delivery efficiency in DOX-CQ/PP, we detected the accumulation of DOX in tumor sites, serum, urine and organs, including heart, liver, lung, kidney and spleen by HPLC. Compared to free DOX injection, MPEG-PLA encapsulation successfully increased the drug accumulation in tumor tissues, while reducing the drug concentrations in normal organs. And co-encapsulating CQ further enhance the phenomenon (Figure 4M), which might result from the selectively release of drugs induced by pH.
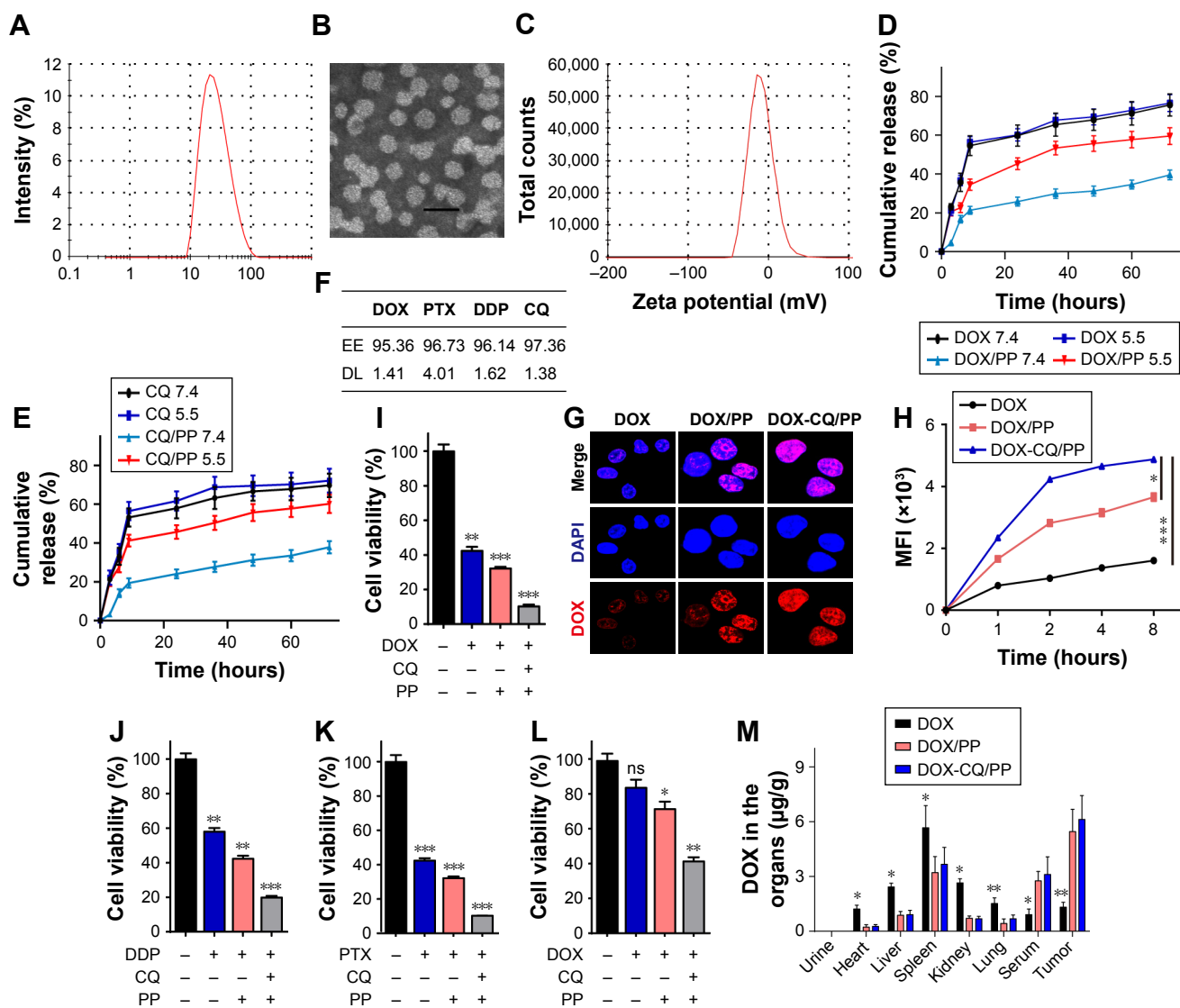
Figure 4 MPEG-PLA nanoparticles encapsulated CQ and DOX enhanced cell apoptosis in vitro and drug accumulation in tumor sites in vivo.

Notes: (**A**) Size distribution spectrum of DOX- and CQ-loaded MPEG-PLA nanoparticles was examined. (**B**) TEM image of DOX- and CQ-loaded MPEG-PLA nanoparticles was shown (Scale bar, 40 nm). (**C**) Zeta potential spectrum of DOX- and CQ-loaded MPEG-PLA micelles. (**D**) Drug release of free DOX and DOX-CQ/PP under different pH conditions (pH 5.5 and pH 7.4) (n=3). (**E**) Drug release of free CQ and DOX-CQ/PP under different pH conditions (pH 5.5 and pH 7.4) (n=3). (**F**) The EE and DL of CQ/DOX/DDP/PTX encapsulated by MPEG-PLA were examined. (**G**) A2780 cells were treated with DOX (1 μM), DOX/PP (DOX concentration 1 μM) and DOX-CQ/PP for 4 hours. The drug uptake was detected by concofol. (**H**) A2780 cells were treated with DOX (1 μM), MPEG-PLA encapsulated DOX (DOX concentration 1 μM) with or without CQ (10 μM). The MFI of the A2780 treated with DOX (1 μM), MPEG-PLA encapsulated DOX (DOX concentration 1 μM) with or without CQ (10 μM) was detected by flow cytometry at different time points. (**I**) The cell viability of A2780 cells treated with PBS, DOX (0.1 μM), DOX/PP (DOX concentration 0.1 μM), and DOX-CQ/PP (DOX concentration 0.1 μM and CQ concentration 10 μM) for 48 hours. (**J**) The cell viability of A2780 cells treated with PBS, DDP (20 μM), DDP/PP (DDP concentration 20 μM) and DDP-CQ/PP (DDP concentration 20 μM and CQ concentration 10 μM). (**K**) The cell viability of A2780 cells treated with PBS, PTX (4 μM), PTX/PP (PTX concentration 4 μM) and PTX-CQ/PP (PTX concentration 4 μM and CQ concentration 10 μM) for 48 hours. (**L**) The cell viability of A2780/DOX^R cells treated with PBS, DOX (0.1 μM), DOX/PP (DOX concentration 0.1 μM) and DOX-CQ/PP (DOX concentration 0.1 μM and CQ concentration 10 μM) for 48 hours. (**M**) Nude mice bearing A2780 cells treated with DOX (5 mg/kg), DOX/PP (DOX concentration 5 mg/kg) and DOX-CQ/PP (DOX concentration 5 mg/kg, CQ concentration 5 mg/kg) every 2 days for 10 days, then sacrificed the mice and obtained blood, tumor tissue and organs. HPLC was used to detect the concentration of DOX (n=6). PP was short for MPEG-PLA. *$P < 0.05$; **$P < 0.01$; ***$P < 0.001$.

Abbreviations: CQ, chloroquine; DL, drug loading; DOX, doxorubicin; EE, encapsulation efficiency; MFI, mean fluorescence intensity; MPEG-PLA, methoxy poly(ethylene glycol)-poly(L-lactic acid); ns, not statistically significant; TEM, transmission electron microscope.

Furthermore, the MEPG-PLA encapsulation also prolonged the drug circulation in peripheral blood, which could efficiently slow the drug release and metabolism, leading to sustained tumor suppression and reduced organ damages.

Together, these results suggested that MPEG-PLA nanoparticles could successfully encapsulate the CQ and DOX, resulting in an improved drug delivery system with enhanced anticancer effects and reduced systemic toxicity.

Encapsulation of CQ and DOX by MPEG-PLA nanoparticles enhanced killing efficiency and reduced systemic toxicity in vivo

Furthermore, we investigated the killing efficacy of MPEG-PLA encapsulated DOX with or without CQ in vivo. Herein, we established the nude mice models bearing A2780 cells and treated with DDP/PP, DDP, MPEG-PLA and PBS. Compared with PBS group, DDP showed limited tumor growth inhibition and DDP/PP exhibited stronger tumor remission, while MPEG-PLA alone showed no inhibition on tumor volume (Figure 5A, left). Consistently, DDP/PP treatment could prolong the survival time compared with other groups, with significant differences (Figure 5A, right). Similar results were obtained in DOX/PP and PTX/PP on mice bearing A2780 cells (Figure 5B and C). These results suggested that encapsulation of drugs by MPEG-PLA could increase the anticancer effects and prolong survival time. Furthermore, we evaluated the killing efficacy of drugs combining with CQ encapsulated by MPEG-PLA on mice

bearing A2780 cells. Accordingly, we observed that DDP and CQ treatment showed significant tumor remission, and MPEG-PLA encapsulation could further elevate the killing ability (Figure 5D, left). Consistently, DDP-CQ/PP treatment could remarkably prolong the survival time (Figure 5D, right). Similarly, encapsulated DOX-CQ and PTX-CQ to treat mice bearing A2780 cells obtained same trends in tumor inhibition and survival time (Figure 5E and F). In addition, we established mice models bearing A2780/DOX^R cells and investigated whether DOX-CQ/PP could reverse the drug resistance. As expected, we observed remarkable tumor inhibition in DOX-CQ treatment group and enhanced killing ability in MPEG-PLA encapsulating DOX and CQ groups (Figure 5G, left). And DOX-CQ/PP treatment could prolong the survival time (Figure 5G, right). These data suggested that MPEG-PLA encapsulating DOX and CQ could also reverse the drug resistance in ovarian cancer treatment. Except for tumor remission efficiency, the side effect induced by chemotherapeutic agents is a pivotal index in clinic treatment. In this study,
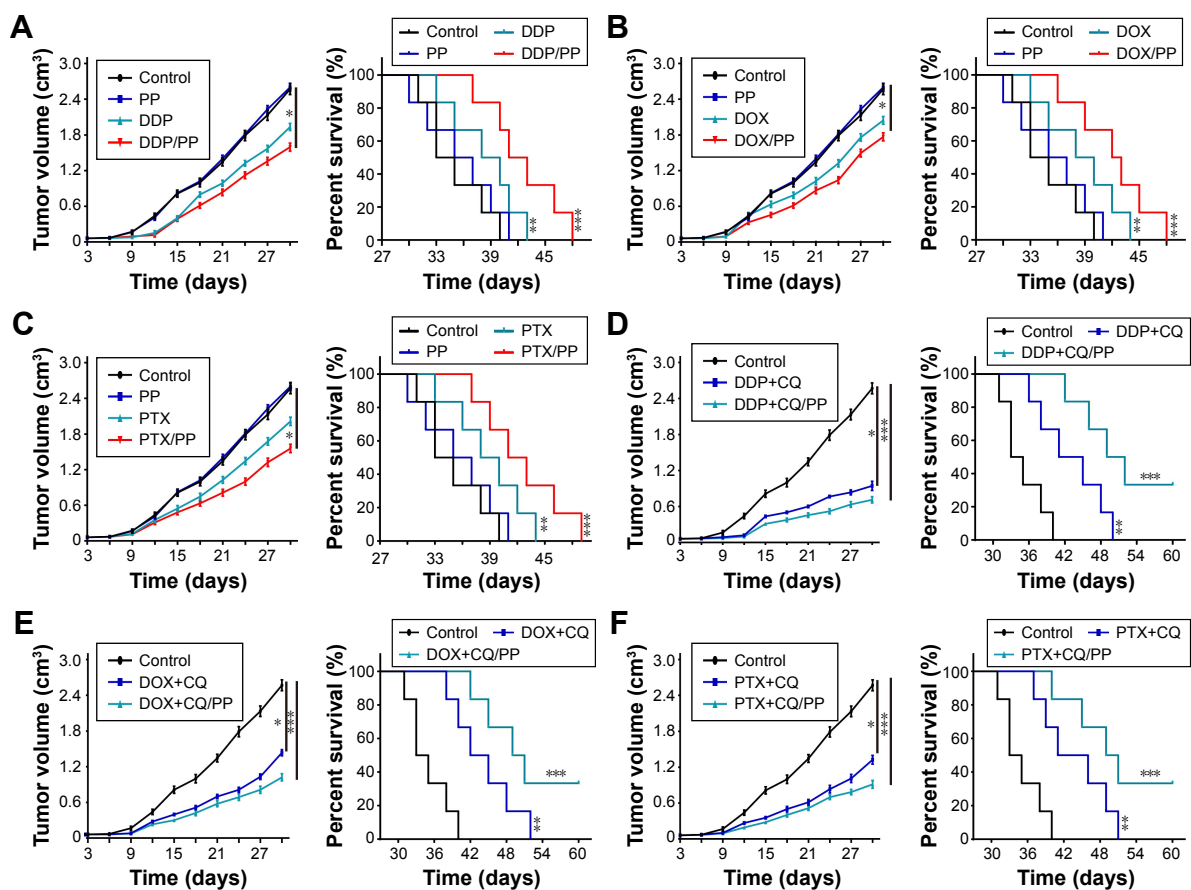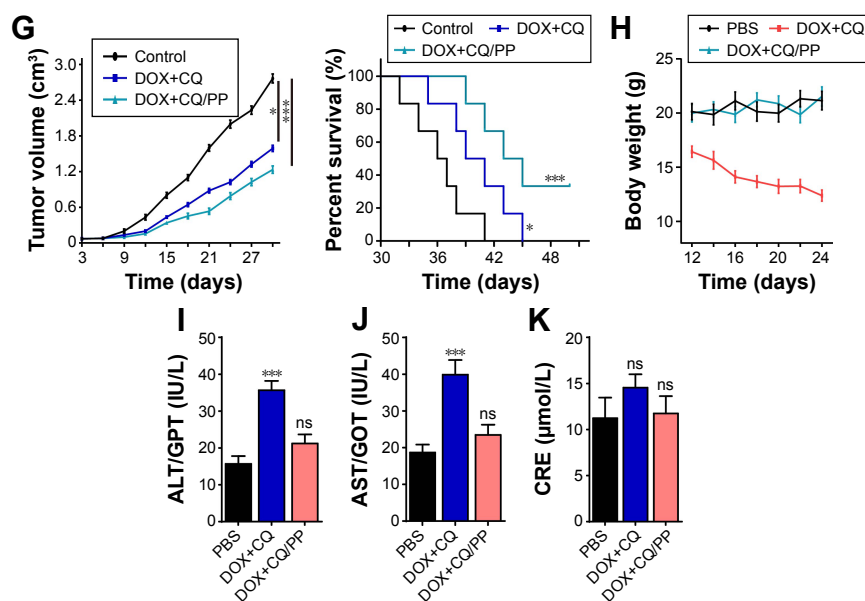

Figure 5 (*Continued*)

Figure 5 Encapsulated CQ and DOX by MPEG-PLA nanoparticles enhanced killing efficiency and reduced systemic toxicity in vivo.
Notes: (**A**) Tumor volume of nude mice model bearing A2780 cells treated with PBS, MPEG-PLA, DDP (6 mg/kg) or DDP/PP (DDP concentration, 6 mg/kg) were measured (n=6) (left). Survival time of nude mice model bearing A2780 cells treated with PBS, MPEG-PLA, DDP (6 mg/kg) or DDP/PP (DDP concentration, 5 mg/kg) in each group (n=6) (right). (**B**) Tumor volume of nude mice model bearing A2780 cells treated with PBS, MPEG-PLA, DOX (5 mg/kg) or DOX/PP (DOX concentration, 5 mg/kg) were measured (n=6) (left). Survival time of nude mice model bearing A2780 cells treated with PBS, MPEG-PLA, DOX (5 mg/kg) or DOX/PP (DOX concentration, 5 mg/kg) in each group (n=6) (right). (**C**) Tumor volume of nude mice model bearing A2780 cells treated with PBS, MPEG-PLA, PTX (15 mg/kg) or PTX/PP (PTX concentration, 15 mg/kg) were measured (n=6) (left). Survival time of nude mice model bearing A2780 cells treated with PBS, MPEG-PLA, PTX (15 mg/kg) or PTX/PP (PTX concentration, 15 mg/kg) in each group (n=6) (right). (**D**) Tumor volume of nude mice model bearing A2780 cells treated with PBS, DDP (6 mg/kg) combining with CQ (5 mg/kg) or DDP-CQ/PP (DDP concentration, 6 mg/kg and CQ, 5 mg/kg) were measured (n=6) (left). Survival time of nude mice model bearing A2780 cells treated with PBS, DDP (6 mg/kg) combining with CQ (5 mg/kg) or DDP-CQ/PP (DDP concentration, 6 mg/kg and CQ, 5 mg/kg) in each group (n=6) (right). (**E**) Tumor volume of nude mice model bearing A2780 cells treated with PBS, DOX (5 mg/kg) combining with CQ (5 mg/kg) or DOX-CQ/PP (DOX concentration, 5 mg/kg and CQ, 5 mg/kg) were measured (n=6) (left). Survival time of nude mice model bearing A2780 cells treated with PBS, DOX (5 mg/kg) combining with CQ (5 mg/kg) or DOX-CQ/PP (DOX concentration, 5 mg/kg and CQ, 5 mg/kg) in each group (n=6) (right). (**F**) Tumor volume of nude mice model bearing A2780 cells treated with PBS, PTX (15 mg/kg) combining with CQ (5 mg/kg) or PTX-CQ/PP (PTX concentration, 15 mg/kg and CQ, 5 mg/kg) were measured (n=6) (left). Survival time of nude mice model bearing A2780 cells treated with PBS, PTX (15 mg/kg) combining with CQ (5 mg/kg) or PTX-CQ/PP (PTX concentration, 15 mg/kg and CQ, 5 mg/kg) in each group (n=6) (right). (**G**) Tumor volume of nude mice model bearing A2780/DOX^R cells treated with PBS, MPEG-PLA, DOX (5 mg/kg) or DOX/PP (DOX concentration, 5 mg/kg) were measured (n=6) (left). Survival time of nude mice model bearing A2780 cells treated with PBS, MPEG-PLA, DOX (5 mg/kg) or DOX/PP (DOX concentration, 5 mg/kg) in each group (n=6) (right). (**H**) The body weight of C57 mice was measured in control, DOX-CQ and DOX-CQ/PP groups (n=6). (**I**) The levels of alanine aminotransferase/glutamic-pyruvic transaminase (ALT/GPT) were detected in C57 mice received DOX (5 mg/kg)-CQ (5 mg/kg) or DOX-CQ/PP (n=6). (**J**) The levels of aspartate aminotransferase/glutamic oxalacetic transaminase (AST/GOT) were detected in in C57 mice received DOX (5 mg/kg)–(5 mg/kg) or DOX-CQ/PP. (**K**) The concentrations of CRE were detected in C57 mice received DOX (5 mg/kg) with or without CQ (5 mg/kg). PP was short for MPEG-PLA. *$P<0.05$; **$P<0.01$; ***$P<0.001$.
Abbreviations: CQ, chloroquine; DOX, doxorubicin; MPEG-PLA, methoxy poly(ethylene glycol)-poly(L-lactic acid); CRE, creatinine; ns, not statistically significant.

we also detected the body weight and functions of liver and kidney on normal C57 mice. Herein, the weight loss induced by CQ and DOX was relieved after MEPG-PLA encapsulation (Figure 5H). Furthermore, our results showed that DOX-CQ treatment resulted in significant toxicity in liver (Figure 5I and J) and limited damage in kidney (Figure 5K). Also, we constructed nude mice models bearing A2780 cells and examined the side effects data. Here, we observed that DOX-CQ delivered by MPEG-PLA nanoparticles relieved the weight loss induced by free DOX-CQ treatment (Figure S2A). Though free DOX-CQ treatment induced slight liver damage, nanoparticle delivery system could reduce the CRE level (Figure S2B). Besides, MPEG-PLA encapsulation successfully reversed the kidney damage induced by free drugs (Figure S2C and D). Together, these results indicated that MPEG-PLA nanoparticles could enhance the killing ability of chemotherapy in vivo, along with reduced side effects.

Discussion

In our study, we revealed that CQ significantly elevated the sensitivity of ovarian cancer cells to chemotherapeutic agents. We found that CQ could facilitate the cytotoxicity of drugs through the reverse of drug sequestration induced by lysosomes. To further improve the pharmacokinetics profiles and reduce the organ damages caused by agents, we designed the MPEG-PLA nanoparticles to co-encapsulate the DOX and CQ for an improved delivery system, resulting in enhanced anticancer effects and reduced systemic toxicity. These findings defined CQ as a promising chemosensitizer and co-encapsulation of DOX and CQ could potentially enhance the efficacy of ovarian cancer clinical treatment.

Chemotherapy is the standard used method in ovarian cancer treatments. However, increasing evidence revealed that chemotherapeutic agents induced limited anticancer effects along with serve side effects.[19] Thus, innovative chemosensitizers to elevate the cytotoxicity of chemotherapeutic agents to tumor cells are urgently needed. Several reports have demonstrated that some chemosensitizers, such as verapamil,[20] could efficiently enhance the cytotoxicity of chemotherapy, resulting in prolonged survival time in mice mouse models.[21] However, the unavoidable side effects, such as kidney damages, caused by the combination of sensitizers and drugs remained to be major hurdle. Furthermore, the poor pharmacokinetics profiles of sensitizers and drugs also limit the application of chemosensitizers in clinic cancer treatment. In our studies, we found that CQ served as a chemosensitizer to increase the sensitivity of ovarian cancer cells to various chemotherapeutic agents. In our studies, CQ served as a lysosomes inhibitor, which efficiently reversed the drug degradation and sequestration effects induced by lysosomes, leading to the enhanced tumor suppression of chemotherapeutic agents. However, the potential systemic toxicity caused by CQ or chemotherapeutic agents is still unavoidable.

Herein, we improved the drug delivery system to facilitate the drug aggregation in tumor sites, along with improved pharmacokinetics profiles induced by MPEG-PLA encapsulation, leading to enhanced anticancer effects and reduced systemic toxicity. Compared to traditional nanoparticles based on drug delivery systems, the CQ- and DOX-loaded MPEG-PLA nanoparticles had an average size of 25 nm with a high stability and low clearance rate, which is more suitable for drug delivery in vivo compared with those carriers with a large size such as liposome.[22] These characters were preferred by tumor tissues due to the EPR effects and selected release of drugs induced by environment pH. Traditional nanocarriers, such as hydrophilic polymer (polyethylene glycol)[23] and liposomes,[24] have demonstrated to be able to efficiently enhance the tumor suppression in vivo. However, potential toxicity and the lacking safety evaluation limited the application of those nanocarriers. The MPEG-PLA nanoparticles composed of degradable polyethylene glycol and polylactic acid, which were approved by the US Food and Drug Administration, ensure the safety as drug delivery carriers.[25] Also, the codelivery of CQ and DOX by nanoparticles enables the tumor cells to uptake the CQ and DOX simultaneously, which efficiently improve the cytotoxicity induced by sensitization effects. However, the successful drug encapsulation is limited by various factors, including the drug solubility, the EE and the DL. Some codelivery system, DOX and siRNA co-loaded mesoporous silica nanoparticles[26] or DOX and verapamil co-loaded hydrogel nanoparticles,[27] are limited by the targeted drugs and could not be applied for other chemotherapeutic agents. Our MPEG-PLA nanoparticle based on codelivery of CQ and chemotherapeutic drugs exhibits great potential for use in the various chemotherapeutic agents, such as PTX and DDP, which provide a favorable approach to achieve an sensitization effects in other chemotherapeutic agents.[28]

Traditional chemotherapy reveals severe side effects, along with the risk of failed tumor suppression and development of drug resistance. And the potential side effects and the poor pharmacokinetics profiles limited the application of chemosensitizers. Thus, co-encapsulation of CQ and DOX by MPEG-PLA has unique advantages: 1) the chemosensitizer we used, CQ, could effectively efficiently sensitize ovarian cancer cells at a low dose compared with traditional chemosensitizers; 2) CQ functioned through increasing the lysosome pH to inhibit the drug degradation effects induced by lysosomes and reverse the drug sequestration effects caused by P-gp. 3) Co-encapsulation of CQ and DOX by MPEG-PLA efficiently reduced the potential toxicity caused by the combination of DOX and CQ, along with enhanced anticancer effects caused by improved pharmacokinetics profiles. 4) Similar sensitization effects were observed in drug-resistant ovarian cancer cells, indicating the potential application in drug-resistant cancer therapy. These advantages further strengthen CQ and DOX co-loaded MPEG-PLA nanoparticles as an ideal strategy in ovarian cancer treatment.

Conclusion

The data presented in this study clearly showed that CQ, increasing lysosome pH value and changing lysosomes functions in cancer cell, could be used as a chemosensitizer to enhance the therapeutic effects of ovarian cancer. And co-encapsulation of CQ and chemotherapeutic agents leaded to elevated anticancer effects and improved outcomes, which may be presented as a promising strategy in the treatment of ovarian cancer patients in the clinic.

Disclosure

The authors report no conflicts of interest in this work.

References

1. Patch AM, Christie EL, Etemadmoghadam D, et al. Whole-genome characterization of chemoresistant ovarian cancer. *Nature*. 2015;521(7553): 489–494.

2. Beusterien K, Grinspan J, Kuchuk I, et al. Use of conjoint analysis to assess breast cancer patient preferences for chemotherapy side effects. *Oncologist*. 2014;19(2):127–134.

3. Liu JF, Barry WT, Birrer M, et al. Combination cediranib and olaparib versus olaparib alone for women with recurrent platinum-sensitive ovarian cancer: a randomised phase 2 study. *Lancet Oncol*. 2014; 15(11):1207–1214.

4. Zhitomirsky B, Assaraf YG. Lysosomes as mediators of drug resistance in cancer. *Drug Resist Updat*. 2016;24:23–33.

5. Lucien F, Pelletier PP, Lavoie RR, et al. Hypoxia-induced mobilization of NHE6 to the plasma membrane triggers endosome hyperacidification and chemoresistance. *Nat Commun*. 2017;8(15884):15884.

6. Seront E, Boidot R, Bouzin C, et al. Tumour hypoxia determines the potential of combining mTOR and autophagy inhibitors to treat mammary tumours. *Br J Cancer*. 2013;109(10):2597–2606.

7. Hasima N, Ozpolat B. Regulation of autophagy by polyphenolic compounds as a potential therapeutic strategy for cancer. *Cell Death Dis*. 2014;5(5):467:e1509.

8. Tian G, Zheng X, Zhang X, et al. TPGS-stabilized NaYbF4:Er upconversion nanoparticles for dual-modal fluorescent/CT imaging and anticancer drug delivery to overcome multi-drug resistance. *Biomaterials*. 2015;40:107–116.

9. Lee PC, Lee HJ, Kakadiya R, Sanjiv K, Su TL, Lee TC. Multidrug-resistant cells overexpressing P-glycoprotein are susceptible to DNA crosslinking agents due to attenuated Src/nuclear EGFR cascade-activated DNA repair activity. *Oncogene*. 2013;32(9):1144–1154.

10. Adar Y, Stark M, Bram EE, et al. Imidazoacridinone-dependent lysosomal photodestruction: a pharmacological Trojan horse approach to eradicate multidrug-resistant cancers. *Cell Death Dis*. 2012; 3(3):30:e293.

11. Yan X, Yang L, Feng G, et al. Lup-20(29)-en-3β,28-di-yl-nitrooxy acetate affects MCF-7 proliferation through the crosstalk between apoptosis and autophagy in mitochondria. *Cell Death Dis*. 2018;9(2):017–255.

12. Li X, Rydzewski N, Hider A, et al. A molecular mechanism to regulate lysosome motility for lysosome positioning and tubulation. *Nat Cell Biol*. 2016;18(4):404–417.

13. Senapati S, Mahanta AK, Kumar S, Maiti P. Controlled drug delivery vehicles for cancer treatment and their performance. *Signal Transduct Target Ther*. 2018;3(7):017–0004.

14. Ambudkar SV, Kimchi-Sarfaty C, Sauna ZE, Gottesman MM. P-glycoprotein: from genomics to mechanism. *Oncogene*. 2003;22(47): 7468–7485.

15. Tutt A, Tovey H, Cheang MCU, et al. Carboplatin in BRCA1/2-mutated and triple-negative breast cancer BRCAness subgroups: the TNT Trial. *Nat Med*. 2018;24(5):628–637.

16. Chen LX, Ni XL, Zhang H, et al. Preparation, characterization, in vitro and in vivo anti-tumor effect of thalidomide nanoparticles on lung cancer. *Int J Nanomedicine*. 2018;13:2463–2476.

17. Kebebe D, Liu Y, Wu Y, Vilakhamxay M, Liu Z, Li J. Tumor-targeting delivery of herb-based drugs with cell-penetrating/tumor-targeting peptide-modified nanocarriers. *Int J Nanomedicine*. 2018;13: 1425–1442.

18. Zhou L, Duan X, Zeng S, et al. Codelivery of SH-aspirin and curcumin by mPEG-PLGA nanoparticles enhanced antitumor activity by inducing mitochondrial apoptosis. *Int J Nanomedicine*. 2015;10:5205–5218.

19. Rodríguez-Razón CM, Yañez-Sánchez I, Ramos-Santillan VO, et al. Adhesion, proliferation, and apoptosis in different molecular portraits of breast cancer treated with silver nanoparticles and its pathway-network analysis. *Int J Nanomedicine*. 2018;13:1081–1095.

20. Wang Y, Li Y, Wang D, et al. Response of heterogeneous cancer cells on targeted nanoparticles. *Nanomedicine*. 2016;12(7):2127–2137.

21. Nóbrega-Pereira S, Caiado F, Carvalho T, et al. VEGFR2-mediated reprogramming of mitochondrial metabolism regulates the sensitivity of acute myeloid leukemia to chemotherapy. *Cancer Res*. 2018;78(3): 731–741.

22. Allen TM, Cullis PR. Liposomal drug delivery systems: from concept to clinical applications. *Adv Drug Deliv Rev*. 2013;65(1):36–48.

23. Davis ME, Zuckerman JE, Choi CH, et al. Evidence of RNAi in humans from systemically administered siRNA via targeted nanoparticles. *Nature*. 2010;464(7291):1067–1070.

24. Maruyama K. Intracellular targeting delivery of liposomal drugs to solid tumors based on EPR effects. *Adv Drug Deliv Rev*. 2011;63(3): 161–169.

25. Huang S, Yu X, Yang L, et al. The efficacy of nimodipine drug delivery using mPEG-PLA micelles and mPEG-PLA/TPGS mixed micelles. *Eur J Pharm Sci*. 2014;63:187–198.

26. Meng H, Mai WX, Zhang H, et al. Codelivery of an optimal drug/ siRNA combination using mesoporous silica nanoparticles to overcome drug resistance in breast cancer in vitro and in vivo. *ACS Nano*. 2013; 7(2):994–1005.

27. Qin M, Lee YE, Ray A, Kopelman R. Overcoming cancer multidrug resistance by codelivery of DOX and verapamil with hydrogel nanoparticles. *Macromol Biosci*. 2014;14(8):1106–1115.

28. Dong Y, Feng SS. Methoxy poly(ethylene glycol)-poly(lactide) (MPEG-PLA) nanoparticles for controlled delivery of anticancer drugs. *Biomaterials*. 2004;25(14):2843–2849.

Supplementary materials
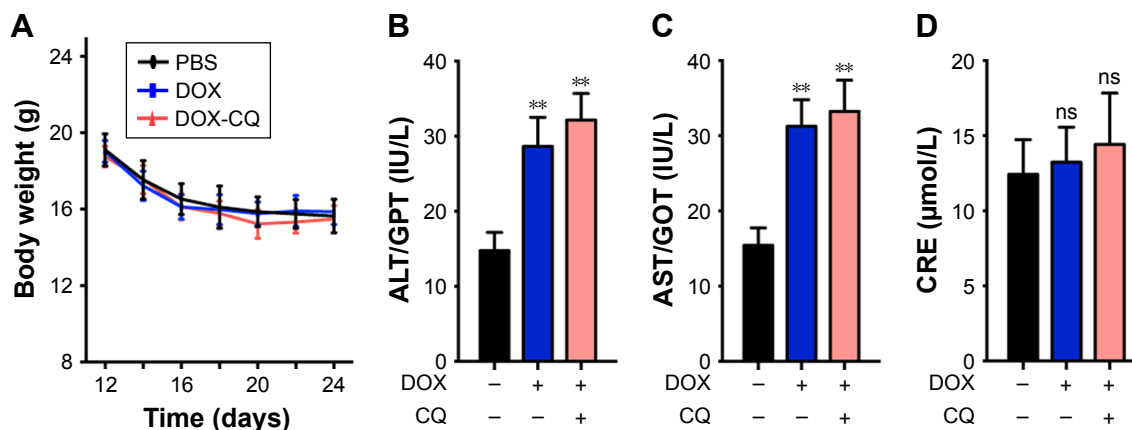
Figure S1 (Attached to Figure 3) (**A**) The body weight of nude mice bearing A2780 cells was measured in control, DOX and DOX-CQ groups (n=6). (**B**) The levels of alanine aminotransferase/glutamic-pyruvic transaminase (ALT/GPT) were detected in nude mice bearing A2780 cells received DOX (5 mg/kg) with or without CQ (5 mg/kg) (n=6). (**C**) The levels of aspartate aminotransferase/glutamic oxalacetic transaminase (AST/GOT) were detected in nude mice bearing A2780 cells received DOX (5 mg/kg) with or without CQ (5 mg/kg). (**D**) The concentrations of CRE were detected in nude mice bearing A2780 cells received DOX (5 mg/kg) with or without CQ (5 mg/kg). **$P < 0.01$.
Abbreviations: CQ, chloroquine; CRE, creatinine; DOX, doxorubicin; ns, not statistically significant.
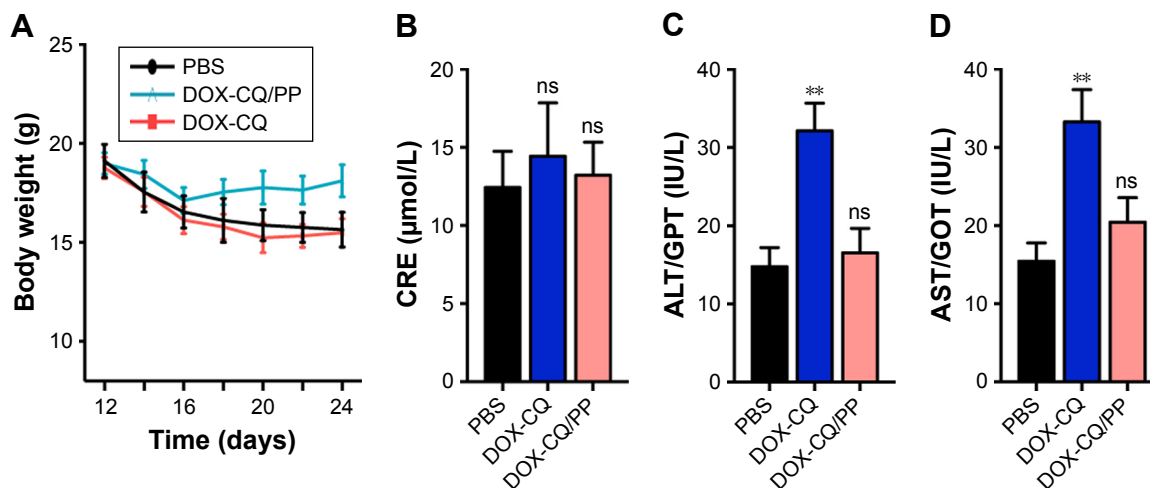
Figure S2 (Attached to Figure 5) (**A**) The body weight of nude mice bearing A2780 cells was measured in control, DOX-CQ and DOX-CQ/PP groups (n=6). (**B**) The levels of alanine aminotransferase/glutamic-pyruvic transaminase (ALT/GPT) were detected in nude mice bearing A2780 cells received DOX (5 mg/kg)-CQ (5 mg/kg) or DOX-CQ/PP (n=6). (**C**) The levels of aspartate aminotransferase/glutamic oxalacetic transaminase (AST/GOT) were detected in nude mice bearing A2780 cells received DOX (5 mg/kg)–(5 mg/kg) or DOX-CQ/PP. (**D**) The concentrations of CRE were detected in nude mice bearing A2780 cells received DOX (5 mg/kg) with or without CQ (5 mg/kg). PP was short for MPEG-PLA. **$P < 0.01$.
Abbreviations: CQ, chloroquine; CRE, creatinine; DOX, doxorubicin; MPEG-PLA, methoxy poly (ethylene glycol)-poly (L-lactic acid); ns, not statistically significant.